

Article

Enhanced Stability of CaO and/or La₂O₃ Promoted Pd/Al₂O₃ Egg-Shell Catalysts in Partial Oxidation of Methane to Syngas

Jinlong Wang ¹, Hongbo Yu ¹, Zhen Ma ^{2,*} and Shenghu Zhou ^{1,*}

¹ Ningbo Institute of Materials Technology & Engineering, Chinese Academy of Sciences, Ningbo 315201, China

² Shanghai Key Laboratory of Atmospheric Particle Pollution and Prevention (LAP³), Department of Environmental Science and Engineering, Fudan University, Shanghai 200433, China

* Authors to whom correspondence should be addressed; E-Mails: zhenma@fudan.edu.cn (Z.M.); zhoush@nimte.ac.cn (S.Z.); Tel.: +86-574-8669-6927; Fax: +86-574-8668-5043.

Received: 17 June 2013; in revised form: 5 July 2013 / Accepted: 9 July 2013 /

Published: 15 July 2013

Abstract: An egg-shell Pd/Al₂O₃ catalyst showed higher activity than a regular Pd/Al₂O₃ catalyst in the partial oxidation of methane to syngas, but a common problem of this reaction is the catalyst deactivation on stream. We attempted to modify the egg-shell catalyst via impregnation with some metal oxide additives. Although the addition of MgO did not show any beneficial effect, the addition of CaO and/or La₂O₃ significantly improved the stability due to the suppression of carbon deposition and phase transformation of the Al₂O₃ support. The catalysts were characterized by X-ray diffraction (XRD), N₂ adsorption-desorption, and thermogravimetric analysis (TGA).

Keywords: palladium catalysts; egg-shell catalyst; partial oxidation of methane; syngas

1. Introduction

Synthesis gas, a valuable feedstock for the synthesis of ammonia, methanol, dimethyl ether, acetic acid, *etc.*, is mainly produced by steam reforming of methane [1–3]. In recent years, increasing attention has been paid to the catalytic partial oxidation of methane (POM) for syngas production because of less energy consumption, lower investment, and more desirable H₂/CO ratio for some downstream processes [4,5].

The catalysts investigated in the POM processes are mainly supported Ni catalysts and noble metal (e.g., Rh, Pt, Ru, Pd, or Ir) catalysts [6,7]. Ni-based catalysts are cheap, but they deactivate easily due to carbon deposition and sintering above 700 °C [8]. Noble metal-based catalysts have much higher activity, and are less susceptible to catalyst deactivation [9,10].

Among noble metal catalysts, Pd catalysts supported on Al₂O₃, SiO₂, MgO, CaO, and rare earth metal oxides have been used in POM [11,12]. The catalytic activity and stability can be improved by adding some promoters. For instance, Ryu *et al.* investigated the addition of CeO₂, BaO, and SrO on the catalytic performance of Pd/Al₂O₃ for POM, and found that the optimum catalyst was a triply promoted Pd catalyst, namely Pd(2)/CeO₂(23)/BaO(11)/SrO(0.8)/Al₂O₃ [13].

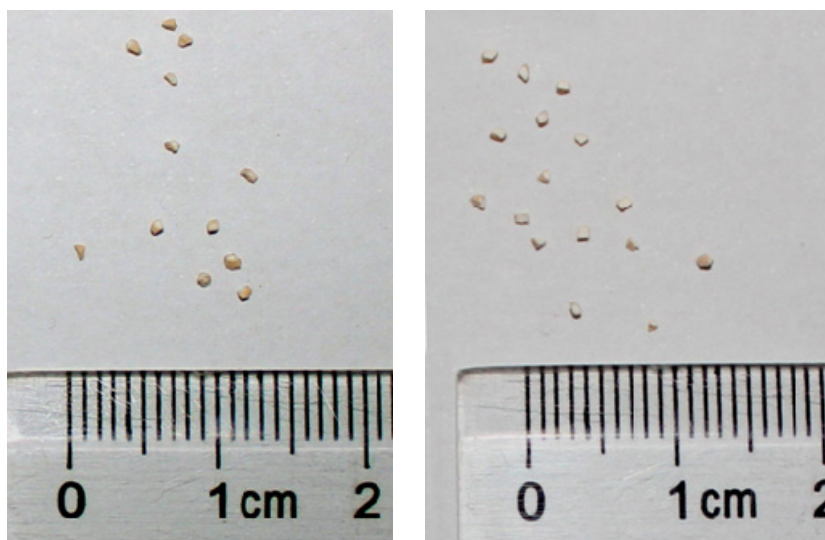
Because POM is performed under very high space velocity, the inner diffusion and reaction inside the pores of the catalysts are limited [14]. Therefore, it is desirable to disperse the active species on the outer surface of the catalyst as far as possible. Egg-shell catalysts can satisfy such a need. Besides, the cost of catalysts can be significantly lowered when adopting the egg shell design. In recent years, Rh [15,16] and Ni [14,17,18] egg-shell catalysts have been investigated in POM. For instance, Chen and co-workers compared the performance of egg-shell and uniform Ni/Al₂O₃ catalysts in POM, and found that egg-shell Ni/Al₂O₃ was more active due to the distribution of nickel component in the outer region of particles [17].

Herein, a Pd/Al₂O₃ egg-shell catalyst and its modified versions were tested in POM. The Pd/Al₂O₃ egg-shell catalyst showed higher activity than a conventional Pd/Al₂O₃, and the addition of CaO and/or La₂O₃ additives can significantly improve the stability on stream due to suppressed carbon deposition and phase transformation of the Al₂O₃ support.

2. Results and Discussion

Figure 1 shows the photos of the prepared egg-shell catalysts before reduction, highlighting the cross section.

Figure 1. Photos showing the cross section of the prepared egg-shell catalysts. Left: PdO/Al₂O₃; Right: PdO/La₂O₃/CaO/Al₂O₃.



The outer surface was dark brown and the inner part of the particles was white, suggesting the accumulation of Pd species on the catalyst surface. The average thickness of the Pd-rich eggshell was approximately 0.2 μm . The catalysts after reduction also showed the egg-shell structure, as seen from the grey-pale black color of the shell while white color at the center.

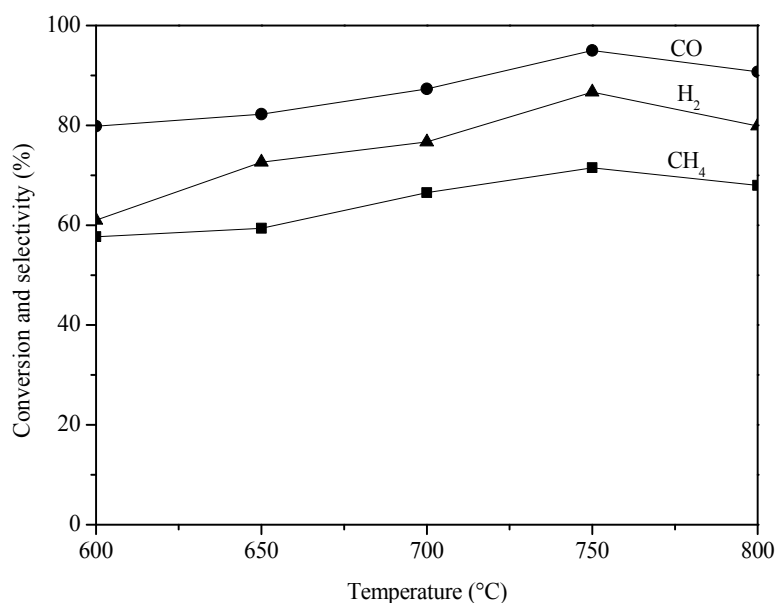
Table 1 summarizes the specific surface areas of support (calcined at 1,000 $^{\circ}\text{C}$) and egg-shell catalyst samples reduced at 750 $^{\circ}\text{C}$. The surface area of Pd/Al₂O₃ egg-shell catalyst was lower than its corresponding Al₂O₃ support, probably due to the blockage of the pores by loading Pd as well as some degradation of the support as a result of the catalyst preparation procedure [19]. The addition of MgO, CaO, La₂O₃, or CaO and La₂O₃ into Pd/Al₂O₃ could retain a higher surface area.

Table 1. Specific surface areas of support (calcined at 1,000 $^{\circ}\text{C}$) and egg-shell catalyst samples reduced at 750 $^{\circ}\text{C}$.

Sample	Specific surface area (m^2/g)
Al ₂ O ₃	118
Pd/Al ₂ O ₃	58
Pd/MgO/Al ₂ O ₃	99
Pd/CaO/Al ₂ O ₃	78
Pd/La ₂ O ₃ /Al ₂ O ₃	78
Pd/La ₂ O ₃ /CaO/Al ₂ O ₃	102

Figure 2 shows the performance of Pd/Al₂O₃ egg-shell catalyst in POM reaction as a function of reaction temperature.

Figure 2. Catalytic performance of Pd/Al₂O₃ egg-shell catalyst in POM reaction at different temperatures.



The CH₄ conversion increased with the reaction temperature and reached 72% at 750 $^{\circ}\text{C}$. For comparison, the CH₄ conversion on a regular Pd/Al₂O₃ catalyst with the same Pd loading (0.2%) was 49% at 750 $^{\circ}\text{C}$, demonstrating the advantage of the egg shell design. The CH₄ conversion on Pd/Al₂O₃

egg-shell catalyst decreased when the reaction temperature was above 750 °C, due to the accelerated carbon deposition at high temperatures.

Figure 3 shows the CH₄ conversion on various egg-shell catalysts at 750 °C as a function of time on stream. The initial CH₄ conversions on these catalysts were comparable, ranging from 67% to 73%. However, the deactivation behaviors were quite different. Pd/Al₂O₃ egg-shell catalyst deactivated quickly on stream, as seen by the dropping of CH₄ conversion from 72% to 40% after operation for 10 h. The addition of MgO barely changed the quick deactivation, whereas the addition of CaO and/or La₂O₃ significantly suppressed the deactivation. In particular, Pd/La₂O₃/CaO/Al₂O₃ egg-shell catalyst showed the best stability: the CH₄ conversion changed from 70% to 62% after operation for 10 h.

Figure 3. Performance of the egg-shell catalysts as a function of time on stream in POM reaction. (a) Pd/Al₂O₃; (b) Pd/MgO/Al₂O₃; (c) Pd/CaO/Al₂O₃; (d) Pd/La₂O₃/Al₂O₃; (e) Pd/La₂O₃/CaO/Al₂O₃.

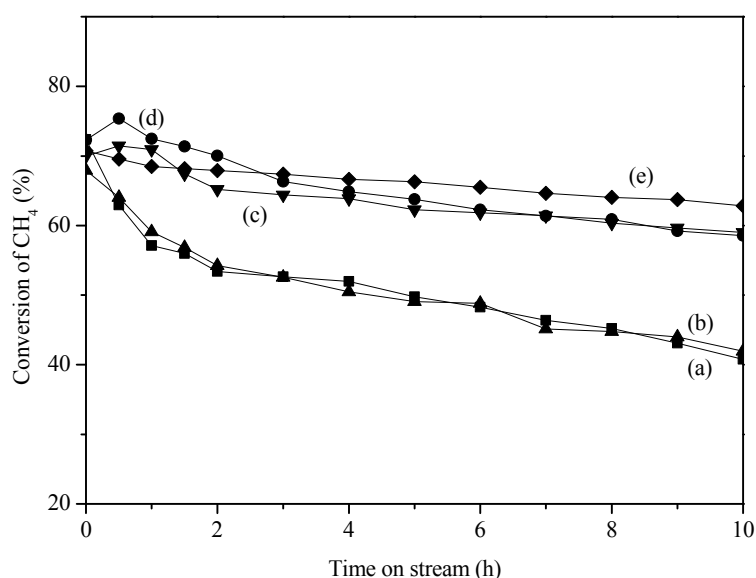


Figure 4. Selectivity to CO and H₂ on Pd/La₂O₃/CaO/Al₂O₃ egg-shell catalyst in POM reaction.

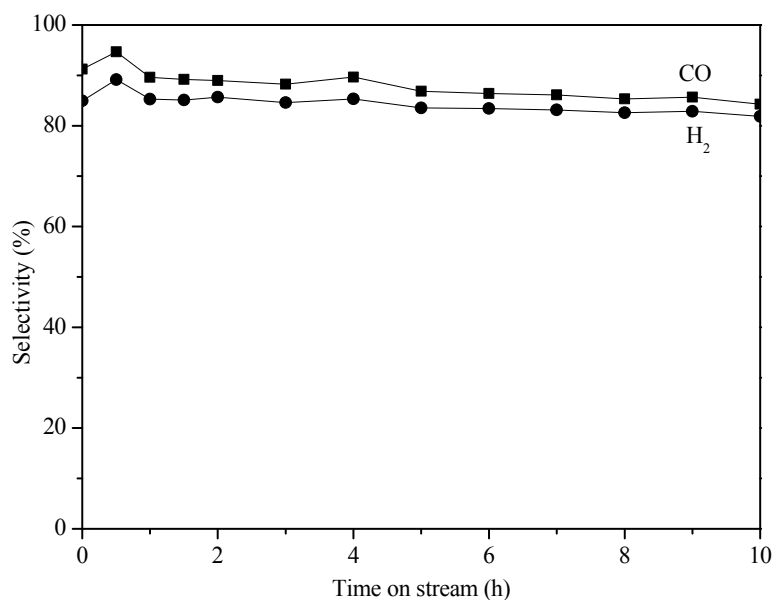
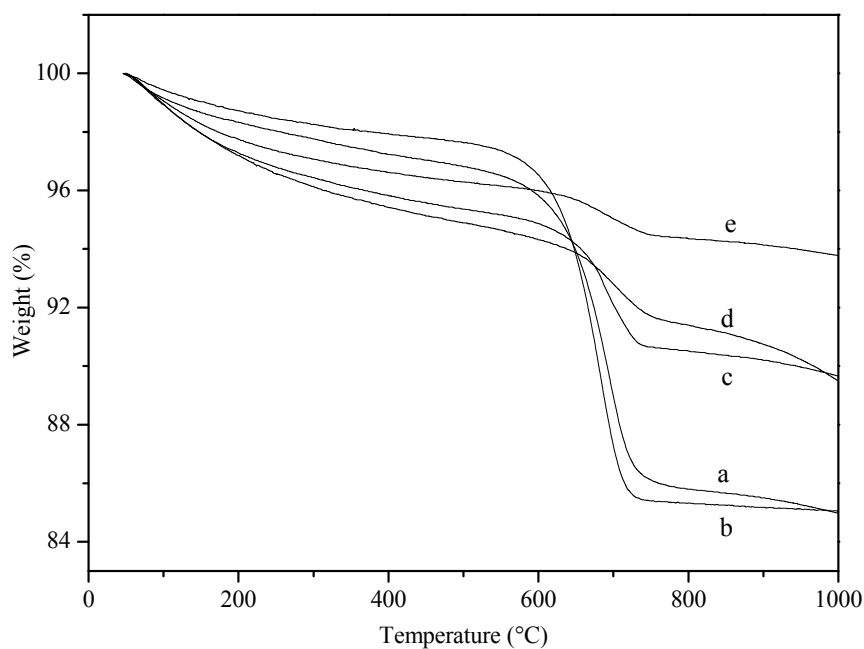


Figure 4 shows the H₂ selectivity and CO selectivity on Pd/La₂O₃/CaO/Al₂O₃ egg-shell catalyst as a function of time on stream. The H₂ selectivity and CO selectivity were about 85% and 91%, respectively.

One reason for catalyst deactivation in the POM process is the deposition of carbon [20]. Indeed, the outer surface of the spent catalysts turned into black, indicating the deposition of carbon during the course of reaction. Therefore, TGA was employed to characterize the spent catalysts. As shown in Figure 5, all the samples showed an obvious weight loss from ca. 600 °C to 750 °C, attributing to the oxidation of deposited carbon, most likely graphitic carbon [21]. Interestingly, the amounts of deposited coke were different with different spent egg-shell catalysts: those on Pd/CaO/Al₂O₃ (4.3%), Pd/La₂O₃/Al₂O₃ (3.4%), and Pd/La₂O₃/CaO/Al₂O₃ (2.0%) were much less than those on Pd/Al₂O₃ (10.7%) and Pd/MgO/Al₂O₃ (12.1%), correlating nicely with the deactivation behaviors.

Figure 5. TG curves of the spent egg-shell catalysts collected after operation for 10 h. (a) Pd/Al₂O₃; (b) Pd/MgO/Al₂O₃; (c) Pd/CaO/Al₂O₃; (d) Pd/La₂O₃/Al₂O₃; (e) Pd/La₂O₃/CaO/Al₂O₃.



Another reason for catalyst deactivation in POM process is the phase transformation of Al₂O₃ [22]. Figure 6 shows the XRD patterns of the support (calcined at 1,000 °C) and egg-shell catalysts reduced at 750 °C. The characteristic diffraction peaks of Al₂O₃ support calcined at 1,000 °C (Figure 6a) were at 31.5°, 32.9°, 36.8°, 39.8°, 45.6°, and 67.3°, corresponding to δ phase (JCPDS 4-877). For Pd/Al₂O₃ catalyst, Pd diffractions were not found since its loading was low (0.2%) and only Al₂O₃ peaks were visible (Figure 6b). Pd/MgO/Al₂O₃ (Figure 6c) showed characteristic diffraction peaks shifted to the direction in lower values of 2θ due to the substitution of Al³⁺ by Mg²⁺ [23]. Pd/CaO/Al₂O₃ (Figure 6d) showed no diffraction peaks of CaO, indicating the high dispersion of CaO in the corresponding catalyst. Peaks at 23.5°, 33.4°, 41.2°, 47.9°, 54.1°, 60.0°, 70.1° in the pattern of Pd/La₂O₃/Al₂O₃ (Figure 6e) were ascribed to the formation of LaAlO₃ (JCPDS 31-22) at high temperatures [24]. The characteristic diffraction peaks of Pd/La₂O₃/CaO/Al₂O₃ (Figure 6f) were similar to those of Pd/La₂O₃/Al₂O₃ (Figure 6e), again without the peaks of CaO species.

Figure 6. XRD patterns of support and egg-shell catalysts reduced at 750 °C. (a) Al₂O₃; (b) Pd/Al₂O₃; (c) Pd/MgO/Al₂O₃; (d) Pd/CaO/Al₂O₃; (e) Pd/La₂O₃/Al₂O₃; (f) Pd/La₂O₃/CaO/Al₂O₃.

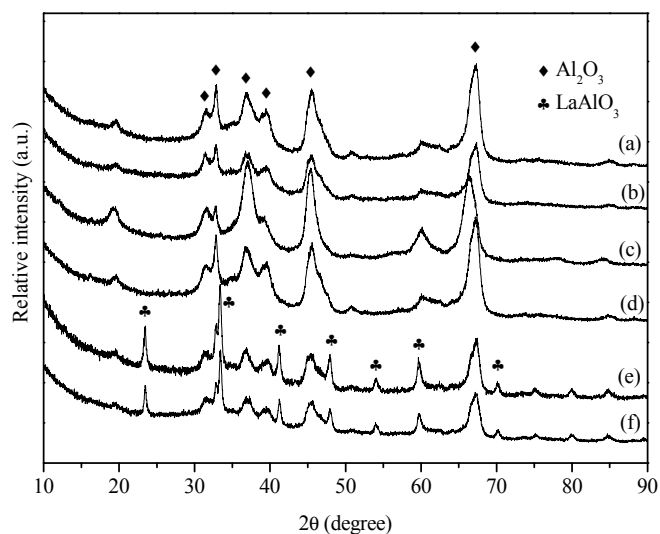
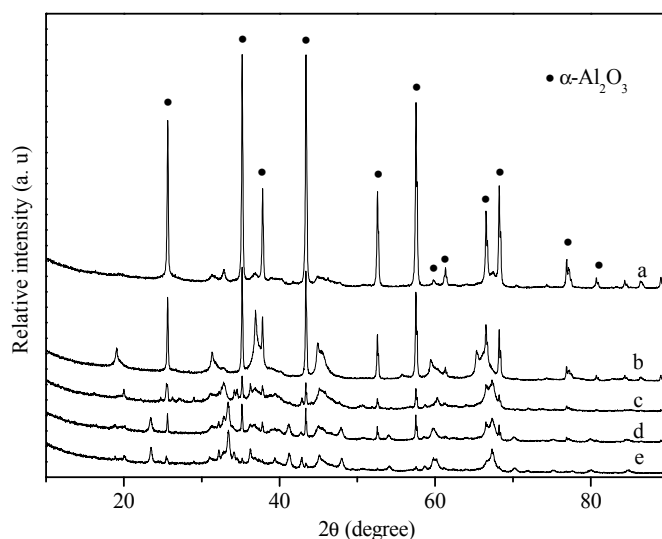


Figure 7 shows the XRD patterns of spent egg-shell catalysts. The diffraction peaks due to α -Al₂O₃ (JCPDS 10-0173) of the used Pd/Al₂O₃ catalyst appeared as shown in Figure 7a. Meanwhile, the diffraction peaks attributed to δ -Al₂O₃ became weaker, indicating the partial transformation from δ -Al₂O₃ into α -Al₂O₃ phase during POM. The addition of Mg slightly impeded the phase transformation of Al₂O₃, whereas the addition of CaO and/or La₂O₃ dramatically inhibited the phase transformation of Al₂O₃. The inhibition of phase transformation of Al₂O₃ by addition of La was probably due to the formation of LaAlO₃ in Al₂O₃ surface. Chen and co-workers found that the deactivation of egg-shell Ni/MgO-Al₂O₃ catalyst in POM was due to the formation of NiO-MgO solution and/or NiAl₂O₄, phase transformation, and sintering [14].

Figure 7. XRD patterns of spent egg-shell catalysts collected after operation for 10 h. (a) Pd/Al₂O₃; (b) Pd/MgO/Al₂O₃; (c) Pd/CaO/Al₂O₃; (d) Pd/La₂O₃/Al₂O₃; (e) Pd/La₂O₃/CaO/Al₂O₃.



3. Experimental

3.1. Catalyst Preparation

Preparation of PdO/Al₂O₃, PdO/MgO/Al₂O₃, and PdO/CaO/Al₂O₃ egg-shell samples: γ -Al₂O₃ Raschig rings purchased from Yixing YiPu Catalyst Company (Yixing, China) were pre-calcined at 1,000 °C for 2 h and then crushed to 1.0–1.3 mm particles. Al₂O₃ particles (5 g) were impregnated with an aqueous solution of Pd precursor by the previously described preparation method [19]. The obtained materials were calcined at 500 °C for 2 h to obtain PdO/Al₂O₃. The PdO/Al₂O₃ samples were impregnated with an aqueous solution of Mg(NO₃)₂ or Ca(NO₃)₂ at room temperature by an incipient impregnation method, and then calcined at 500 °C for 2 h to obtain PdO/MgO/Al₂O₃ and PdO/CaO/Al₂O₃, respectively. For the preparation of PdO/La₂O₃/Al₂O₃ and PdO/La₂O₃/CaO/Al₂O₃, pre-calcined Al₂O₃ particles (5 g) were impregnated with an aqueous solution of La(NO₃)₃ and then calcined to obtain La₂O₃/Al₂O₃ supports. The supports were impregnated with an aqueous solution of Pd precursor by the preparation method provided by [19] and then calcined at 500 °C for 2 h for the preparation of egg-shell PdO/La₂O₃/Al₂O₃ samples. The above PdO/La₂O₃/Al₂O₃ was impregnated with an aqueous solution of Ca(NO₃)₂, and then calcined at 500 °C for 2 h to obtain PdO/La₂O₃/CaO/Al₂O₃. The Pd loading contents were 0.2% (wt %) in all catalysts. The weight ratios of the additive La, Mg, and Ca to Al₂O₃ were 0.1, 0.05, and 0.05, respectively.

3.2. Catalyst Characterization

The powder X-ray diffraction (XRD) patterns were recorded on a Bruker Advance diffractometer (Bruker, Karlsruhe, Germany) with a Cu K α monochromatic radiation operated at 40 kV and 40 mA, using a scanning range 2 θ between 10° and 90°.

The BET surface areas of the support materials and catalysts were measured by N₂ adsorption at –196 °C using a Micromeritics ASAP 2020 instrument (Micromeritics, Norcross, GA, USA). The samples were outgassed under N₂ flow at 300 °C for 2 h before the measurements.

The amount of carbon deposited on the catalysts after reaction was determined on a Pyris Diamond TG instrument (PerkinElmer, Waltham, MA, USA) by heating the samples from room temperature to 1,000 °C (heating rate 10 °C/min) in a flowing air (25 mL/min).

3.3. Catalytic Test

The POM reaction was carried out in a continuous flow reactor apparatus equipped with a quartz tube reactor operated at atmospheric pressure. The flow rate of gases was controlled by mass flow controllers. The catalysts (0.5 g) were firstly reduced in a 60 mL/min H₂ flow at 750 °C for 30 min, then a 60 mL/min Ar flow was introduced to flush the system. Afterwards, a mixture of CH₄ (99.9%, 277.8 mL/min) and O₂ (99.999%, 138.9 mL/min) with a molar ratio of 2:1 at weight hour space velocity (WHSV) of 5×10^4 mL·g⁻¹·h⁻¹ was introduced. The product gases were analyzed online by a gas chromatograph equipped with a TCD detector and TDX-01 packed column. Water was trapped before gases entered the gas chromatograph.

4. Conclusions

A series of Pd/Al₂O₃-based egg-shell catalysts were tested in the partial oxidation of methane. The addition of MgO, CaO, or La₂O₃ additives had no dramatic effect on the initial CH₄ conversion. The addition of MgO additive had no effect on the catalyst stability, whereas the addition of CaO and/or La₂O₃ significantly improved the catalyst stability because they suppressed the formation of carbon deposit and phase transformation of the Al₂O₃ support. More experiments should be done in the future to understand why the addition of certain additives could suppress the deposition of carbon.

Acknowledgments

S.H. Zhou thanks the Ministry of Science and Technology of China (Grant No. 2012DFA40550) for its financial support. Z. Ma acknowledges the financial support by National Natural Science Foundation of China (Grant Nos. 21007011 and 21177028), the Ph.D. Programs Foundation of the Ministry of Education in China (Grant No. 20100071120012), and the Overseas Returnees Start-Up Research Fund of the Ministry of Education in China.

Conflict of Interest

The authors declare no conflict of interest.

References

1. Bitsch-Larsen, A.; Horn, R.; Schmidt, L.D. Catalytic partial oxidation of methane on rhodium and platinum: Spatial profiles at elevated pressure. *Appl. Catal. A* **2008**, *348*, 165–172.
2. Nurunnabi, M.; Mukainakano, Y.; Kado, S.; Li, B.T.; Kunimori, K.; Suzuki, K.; Fujimoto, K.; Tomishige, K. Additive effect of noble metals on NiO-MgO solid solution in oxidative steam reforming of methane under atmospheric and pressurized conditions. *Appl. Catal. A* **2006**, *299*, 145–156.
3. Kikuchi, E.; Chen, Y. Syngas formation by partial oxidation of methane in palladium membrane reactor. *Stud. Surf. Sci. Catal.* **1998**, *119*, 441–446.
4. Qin, D.Y.; Lapszewicz, J.; Jiang, X.Z. Comparison of partial oxidation and steam-CO₂ mixed reforming of CH₄ to syngas on MgO-supported metals. *J. Catal.* **1996**, *159*, 140–149.
5. York, A.P.E.; Xiao, T.C.; Green, M.L.H. Brief overview of the partial oxidation of methane to synthesis gas. *Top. Catal.* **2003**, *22*, 345–358.
6. Enger, B.C.; Lødeng, R.; Holmen, A. A review of catalytic partial oxidation of methane to synthesis gas with emphasis on reaction mechanisms over transition metal catalysts. *Appl. Catal. A* **2008**, *346*, 1–27.
7. Tsang, S.C.; Claridge, J.B.; Green, M.L.H. Recent advances in the conversion of methane to synthesis gas. *Catal. Today* **1995**, *23*, 3–15.
8. Lanza, R.; Velasco, J.A.; Järås, S.G. Recent Developments and Achievements in Partial Oxidation of Methane with and without Addition of Steam. In *Catalysis*; Spivey, J.J., Dooley, K.M., Eds.; The Royal Society of Chemistry: Cambridge, UK, 2011; Volume 23, pp. 50–95.

9. Yang, S.W.; Kondo, J.N.; Hayashi, K.; Hirano, M.; Domen, K.; Hosono, H. Partial oxidation of methane to syngas over promoted C12A7. *Appl. Catal. A* **2004**, *277*, 239–246.
10. Choque, V.; Homs, N.; Cicha-Szot, R.; de la Piscina, P.R. Study of ruthenium supported on Ta₂O₅-ZrO₂ and Nb₂O₅-ZrO₂ as catalysts for the partial oxidation of methane. *Catal. Today* **2009**, *142*, 308–313.
11. Choudhary, V.R.; Prabhakar, B.; Rajput, A.M.; Mamman, A.S. Oxidative conversion of methane to CO and H₂ over Pt or Pd containing alkaline and rare earth oxide catalysts. *Fuel* **1998**, *77*, 1477–1481.
12. Bhattacharya, A.K.; Breach, J.A.; Chand, S.; Ghorai, D.K.; Hartridge, A.; Keary, J.; Mallick, K.K. Selective oxidation of methane to carbon monoxide on supported palladium catalyst. *Appl. Catal. A* **1992**, *80*, L1–L5.
13. Ryu, J.H.; Lee, K.Y.; Kim, H.J.; Yang, J.I.; Jung, H. Promotion of palladium-based catalysts on metal monolith for partial oxidation of methane to syngas. *Appl. Catal. B* **2008**, *80*, 306–312.
14. Qiu, Y.J.; Chen, J.X.; Zhang, J.Y. Effect of calcination temperature on properties of eggshell Ni/MgO-Al₂O₃ catalyst for partial oxidation of methane to syngas. *Catal. Lett.* **2009**, *127*, 312–328.
15. Vella, L.D.; Montini, T.; Specchia, S.; Fornasiero, P. Fixed beds of Rh/Al₂O₃-based catalysts for syngas production in methane SCT-GPO reactors. *Int. J. Hydrogen Energy* **2011**, *36*, 7776–7784.
16. Specchia, S.; Vella, L.D.; de Rogatis, L.; Montini, T.; Specchia, V.; Fornasiero, P. Rh-based catalysts for syngas production via SCT-CPO reactors. *Catal. Today* **2010**, *155*, 101–107.
17. Qiu, Y.J.; Chen, J.X.; Zhang, J.Y. Influence of nickel distribution on properties of spherical catalysts for partial oxidation of methane to synthesis gas. *Catal. Commun.* **2007**, *8*, 508–512.
18. Qiu, Y.J.; Chen, J.X.; Zhang, J.Y. Effects of CeO₂ and CaO composite promoters on the properties of eggshell Ni/MgO-Al₂O₃ catalysts for partial oxidation of methane to syngas. *React. Kinet. Catal. Lett.* **2008**, *94*, 351–357.
19. Liu, Z.N.; Zhou, S.H.; Hou, M.B.; Xie, Z.K.; Zhu, H.Y. First-stage selective hydrogenation catalyst for pyrolysis gasoline. Chinese Patent CN1443829A, 24 September 2003.
20. Dissanayake, D.; Rosynek, M.P.; Kharas, K.C.C.; Lunsford, J.H. Partial oxidation of methane to carbon monoxide and hydrogen over a Ni/Al₂O₃ catalyst. *J. Catal.* **1991**, *132*, 117–127.
21. Zhang, Z.L.; Verykios, X.E. Carbon dioxide reforming of methane to synthesis gas over supported Ni catalysts. *Catal. Today* **1994**, *21*, 589–595.
22. Zhang, Y.H.; Xiong, G.X.; Sheng, S.S.; Yang, W.S. Deactivation studies over NiO/γ-Al₂O₃ catalysts for partial oxidation of methane to syngas. *Catal. Today* **2000**, *63*, 517–522.
23. Jing, S.Y.; Lin, L.B.; Huang, N.K.; Zhang, J.; Lu, Y. Investigation on lattice constants of Mg-Al spinels. *J. Mater. Sci Lett.* **2000**, *19*, 225–227.
24. Shi, C.K.; Zhang, P. Effect of a second metal (Y, K, Ca, Mn or Cu) addition on the carbon dioxide reforming of methane over nanostructured palladium catalysts. *Appl. Catal. B* **2012**, *115–116*, 190–200.

Sample Availability: Samples of the compounds are available from the authors.